ELSEVIER

Polymer 42 (2001) 6031–6041

polymer

www.elsevier.nl/locate/polymer

Miscibility, crystallization and real-time small-angle X-ray scattering investigation of the semicrystalline morphology in thermosetting polymer blends

Q. Guo[a,1], C. Harrats[a], G. Groeninckx[a,*], H. Reynaers[a], M.H.J. Koch[b]

[a]*Department of Chemistry, Laboratory of Macromolecular Structural Chemistry, Catholic University of Leuven (KULeuven), Celestijnenlaan 200F, B-3001 Heverlee, Belgium*

[b]*European Molecular Biology Laboratory, Hamburg Outstation, EMBL c/o DESY, Notkestrasse 85, D-22603 Hamburg, Germany*

Received in revised form 31 December 2000; accepted 29 January 2001

Abstract

The results of the study of a completely miscible thermosetting polymer blend containing a crystallizable component are reported. Blends of poly(ϵ-caprolactone) (PCL) and bisphenol-A-type epoxy resin (ER) cured with 4,4′-methylenebis(3-chloro-2,6-diethylaniline) (MCDEA) were prepared and compared with blends of PCL with uncured bisphenol A-type epoxy resin, i.e. diglycidylether of bisphenol A (DGEBA). The miscibility, crystallization behavior and spherulitic morphology of both uncured DGEBA/PCL blends and MCDEA-cured ER/PCL blends were investigated by differential scanning calorimetry (DSC), optical microscopy, and Fourier-transform infrared (FTIR) spectroscopy. It was found that PCL is completely miscible with both DGEBA and MCDEA-cured ER in the melt and in the amorphous state over the entire composition range, as shown by the existence of a single composition-dependent glass transition temperature (T_g). The overall crystallization rate and crystallinity of PCL in the MCDEA-cured ER/PCL blends decrease much more rapidly with increasing amorphous content than those of the DGEBA/PCL blends. The spherulitic morphology of PCL in both the uncured and the cured blends is characteristic of miscible crystalline/amorphous blends, and the PCL spherulites in these blends are always completely volume-filling. The miscibility of the uncured DGEBA/PCL blends is considered to be due predominately to the entropic contribution, whereas that of the cured ER/PCL blends is due to the enthalpic contribution. FTIR investigations indicated hydrogen bonding interaction between the hydroxyl groups of MCDEA-cured ER and the carbonyl groups of PCL in the cured system, which is an important driving force for the miscibility of the cured ER/PCL blends. Real-time small-angle X-ray scattering (SAXS) experiments revealed that the amorphous cured ER segregated interlamellarly during the crystallization process of PCL, which is considered to result from the low chain mobility of the cured ER in the ER/PCL blends. On the basis of the SAXS results, a model describing the semicrystalline morphology of MCDEA-cured ER/PCL blends is proposed. The amorphous fraction of PCL, the branched ER chains and imperfect ER network are located between PCL lamellae in the crystallized blend.

Keywords: Epoxy resin; Poly(ϵ-caprolactone); Polymer miscibility

1. Introduction

Polymer blends are becoming increasingly important in the polymer industry due to the strong economic incentives arising from their use [1] and large number of scientific papers on thermoplastic polymer blends are published every year. In contrast, the study of thermosetting polymer blends where one component is a crystallizable linear polymer and the other is highly crosslinked has received much less attention [2], and little was published before 1989 [3–5]. Thermodynamic considerations suggest that an increase in the molecular weight for either of the components of a miscible blend should reduce the entropy of mixing. Consequently, phase separation induced by cross-linking is expected for systems with a positive (endothermic) enthalpy of mixing. Since 1989 a series of such thermosetting polymer blends have indeed been reported, and it was found that phase separation occurs as the cross-linking process proceeds [2,5–10]. Miscibility and hydrogen bonding interactions between the components were, however, also observed in a few cases, even for some highly cross-linked blends [2,11–15]. Hydrogen

* Corresponding author. Tel.: +32-16-32-74-40; fax: +32-16-32-79-90.
E-mail address: gabriel.groeninckx@chem.kuleuven.ac.be (G. Groeninckx).

[1] On leave from Department of Polymer Science and Engineering, University of Science and Technology of China, Hefei, China.

0032-3861/01/$ - see front matter
PII: S0032-3861(01)00093-3

bonding was considered to be the driving force for miscibility, and the cause of the exothermic mixing that is the thermodynamic basis of the miscibility in these thermosetting polymer blends.

The complex interrelationship between phase behavior and crosslinking in this type of blend systems has not yet been clarified. Moreover, if one of the components of a thermosetting polymer blend is crystallizable, some fundamental information about crystallization can be obtained, as it is expected that cross-linking will influence the crystallization behavior of the blend.

Epoxy resins represent a major class of thermosetting polymers which are widely used as matrices for composite materials and as structural adhesives [16]; they are amorphous, highly crosslinked polymers and their network structure results in materials with a high modulus and high fracture strength, low creep, and good performance at elevated temperatures. However, their network structure also leads to a low toughness and poor crack resistance. This explains why most studies on blends of epoxy resins with rubbers and thermoplastics are aimed at toughening epoxy resins for various end-use applications. Cured blends of epoxy resins with other polymers are usually multiphase systems; the dispersed phase consists of rubbery or thermoplastic domains and the continuous phase is a crosslinked epoxy resin. One of the most successful methods of improving the toughness of an epoxy resin is to incorporate a second phase of dispersed rubbery particles or thermoplastic domains into its matrix [17].

Noshay and Robeson [3] examined the miscibility of a range of anhydride-cured epoxy resins with poly(ϵ-caprolactone) (PCL) of various low molecular weights and with different end groups. These authors found that, above a critical molecular weight (3000–5000) of PCL, the blends displayed a two-phase structure and that the PCL end groups reacted with the anhydride curing agent to form a type of block copolymer. Clark et al. [4]reported that PCL with an average molecular weight of about 20000 was partially miscible with amine-cured epoxy resins, but immiscible with anhydride-cured epoxy resins. It has been proven, however, that the miscibility of an epoxy resin with a linear polymer strongly depends not only on the molecular weight of the linear component but also on the nature of curing agent [18].

Below we report the results of our investigations on semicrystalline thermosetting polymer blends based on PCL and a bisphenol-A-type epoxy resin (ER), i.e. diglycidylether of bisphenol A (DGEBA), using 4,4′-methylenebis(3-chloro-2,6-diethylaniline) (MCDEA) as curing agent. The PCL used in this study has a high molecular weight ($M_w = 94000$ with $M_w/M_n = 2.79$). Blends of PCL with uncured bisphenol A-type epoxy resin, DGEBA, were also examined for comparison. Complete miscibility of uncured DGEBA/PCL and MCDEA-cured ER/PCL blends is established on the basis of DSC, optical microscopy and Fourier-transform infrared (FTIR) spectroscopy. Real-time small-angle X-ray scattering (SAXS) experiments have been performed to investigate the semicrystalline morphology, which will provide very important information on the crystalline lamellar structure of PCL and segregation of the amorphous MCDEA-cured ER component in this type of polymer blends.

2. Experimental

2.1. Materials and sample preparation

The (PCL) was obtained from Janssen Chemical Company, Ltd., Belgium; it has a weight-average molecular weight M_w of 94000 with $M_w/M_n = 2.79$ when measured by GPC in tetrahydrofuran at room temperature using polystyrene standards. The uncured epoxy resin is diglycidyl ether of bisphenol A (DGEBA) (Epikote 828EL, Shell Company, Netherlands) and has an epoxide equivalent weight of 190. Prior to use, it was degassed under vacuum at 120°C for at least 24 h to remove any volatile impurities. (MCDEA) (Aldrich Inc., USA) was used as curing agent. Uncured DGEBA/PCL blends were prepared by mixing PCL and DGEBA at 90°C for a sufficiently long time and then slowly cooled and kept at room temperature.

To prepare the MCDEA-cured ER/PCL blends, PCL was first dissolved in DGEBA by continuous stirring at 90°C. The curing agent MCDEA was then added to the mixture under continuous stirring until a homogeneous ternary mixture was obtained. MCDEA was used in stoichiometric epoxide/amine ratios. The samples of ternary mixture were cured successively at 130°C for 2 h, 150°C for 2 h and 170°C for 2 h.

2.2. Differential scanning calorimetry

The calorimetric measurements were made on a Perkin–Elmer DSC-7 differential scanning calorimeter in a dry nitrogen atmosphere. Indium and tin standards were used for calibration for low and high temperature regions, respectively. Samples of about 8 mg were placed in the DSC pan. All samples were first heated to 100°C at a rate of 20°C/min (the first heating scan) and were kept at that temperature for 2 min. After quenching the sample to −90°C a second heating scan was conducted at the same heating rate. In order to record the crystallization process from the melt, all the samples were first heated up to 100°C and held for 2 min in the melt; they were then cooled down at a rate of −10°C/min. The midpoint of the slope change of the heat capacity plot of the second heating scan was taken as the glass transition temperature (T_g). The crystallization temperature (T_c) was taken as the minimum of the exothermic peak, whereas the melting temperature (T_m) was taken as the maximum of the endothermic peak. The heat of fusion (ΔH_f) and the heat of crystallization (ΔH_c) were evaluated from the areas of the melting and crystallization peaks, respectively.

2.3. Fourier-transform infrared (FTIR) spectroscopy

FTIR measurements were made with a Perkin–Elmer 2000 Fourier-transform infrared spectrometer for the cured ER/PCL blends. Little lumps scraped from the cured samples were mixed with KBr in a mortar and then ground into fine powder, which was further pressed into thin sheets for FTIR measurements. All spectra were recorded at room temperature and signal-averaged over 64 scans at a resolution of 2 cm^{-1}.

2.4. Morphological observations

The overall morphology of the pure PCL, the DGEBA/PCL blends, as well as the MCDEA-cured ER/PCL blends was investigated by optical microscopy using an Olympus BH2 microscope equipped with cross-polarizers. The samples were placed between two glass covers and crystallized from the melt before observation.

2.5. Real-time SAXS measurements

Time-resolved SAXS measurements were carried out on the double focusing monochromator-mirror camera X33 [19] of the EMBL in HASYLAB on the storage ring DORIS III of the Deutsches Electronen Synchrotron (DESY) in Hamburg. The range of scattering vector $s = 2\sin\theta/\lambda$, where 2θ is the scattering angle and λ the wavlength (0.15 nm), was 0.02–0.3 nm^{-1}. About 1 mm thick samples were sealed between thin (70 μm) aluminum foils and placed in a Mettler FP-82 hot stage mounted in the X-ray beam path. During these experiments, the specimens were first kept at 80°C for 1 min and then cooled at −10°C/min to 25°C, kept at 25°C for 15 s, and then heated to 80°C at 10°C/min. The SAXS patterns were collected every 15 s, corresponding to a temperature increment of 2.5°C. The data were processed using the OTOKO software package [20]. The original SAXS data were smoothed and corrected for background scattering by the subtraction of the pattern of an amorphous sample in the molten state.

The crystalline lamellar and amorphous layer thickness (l_c and l_a) and the long period (L) were obtained from the linear correlation function [21]:

$$\gamma(x) = \frac{\int_0^\infty I(s)s^2 \cos(2\pi xs)\,\mathrm{d}s}{\int_0^\infty I(s)s^2\,\mathrm{d}s} \quad (1)$$

where s is the modulus of the scattering vector and x represents a distance in real space. Prior to integration, the data were extrapolated to high angles assuming sigmoidal changes of the electron density of the crystalline-amorphous phase boundaries:

$$I(s)s^4 = K_p \exp(-4\pi^2\sigma^2 s^2) \quad (2)$$

where K_p is a constant and σ is the standard deviation of the smoothing function used to describe the electron density profile at the interface between amorphous and crystalline regions. The long period L is defined as the sum of the thickness of the lamellar and amorphous layers (l_c and l_a).

3. Results and discussion

3.1. Miscibility and spherulitic morphology of uncured DGEBA/PCL blends

The DGEBA/PCL blends containing 10 wt% or more PCL were opaque at room temperature due to the crystallization of PCL in the blends. All the blends were however transparent just above the melting point of PCL, indicating that PCL and DGEBA are miscible in the molten state. Fig. 1 presents the T_g values of the uncured DGEBA/PCL blends obtained from the DSC thermograms of the quenched samples as a function of their composition (full circles). All the blends display a single, composition dependent T_g, strongly indicating that the two components are miscible in the amorphous state. The broken line in the figure is drawn on the basis of the Fox equation [22]:

$$1/T_g(\text{blend}) = W(\text{DGEBA})/T_g(\text{DGEBA}) + W(\text{PCL})/T_g(\text{PCL}) \quad (3)$$

where T_g(blend) is the glass transition temperature of the blend, T_g(DGEBA) and T_g(PCL) are the T_gs of plain

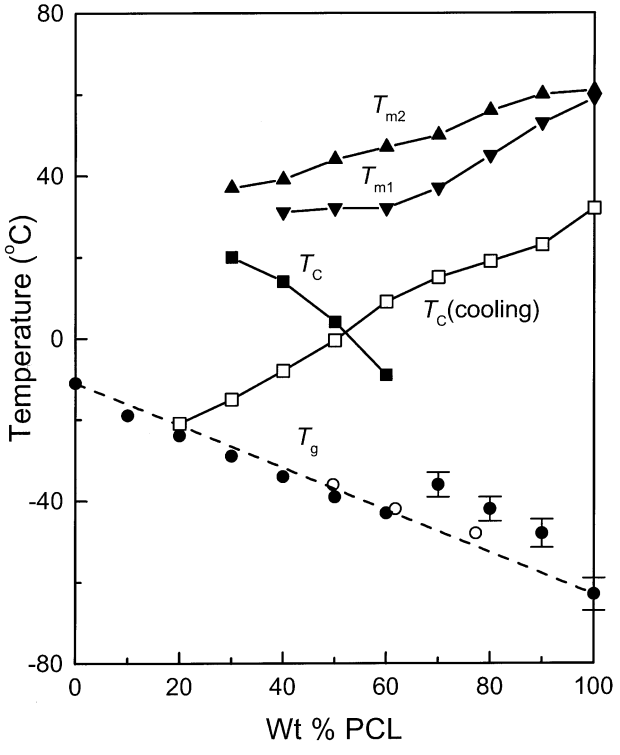

Fig. 1. Thermal transitions of the quenched samples of uncured DGEBA/PCL blends. (●) Experimental T_g versus overall blend composition, (○) T_g versus calculated amorphous composition, (-·-·-) theoretical curve of T_g according to the Fox equation, and (□) T_c(cooling).

DGEBA and PCL, respectively, and W(DGEBA) and W(PCL) represent the weight fractions of DGEBA and PCL.

From Fig. 1 it is noted that for the DGEBA/PCL blends with 70 wt% or more PCL, the values of T_g have a positive deviation from those predicted by the Fox equation, which is considered to be the result of the high crystallinity of PCL. The degree of crystallinity, X_c, was calculated by the following equations:

$$X_c(\text{blend}) = (\Delta H_f - \Delta H_c)/\Delta H_f^o \quad (4)$$

$$X_c(\text{PCL}) = X_c(\text{blend})/W(\text{PCL}) \quad (5)$$

where $\Delta H_f^o = 136$ J/g is the heat of fusion of 100% crystalline PCL [23], ΔH_f is the heat of fusion of the blend and ΔH_c is the heat of crystallization during the same heating scan.

Because of the crystallization of PCL in these blend compositions, the weight fraction of PCL in the amorphous phase, W′(PCL), is not equal to its overall weight fraction in the blend, W(PCL). These quantities are related as follows [24]:

$$W'(\text{PCL}) = (W(\text{PCL}) - X_c(\text{blend}))/(1 - X_c(\text{blend})) \quad (6)$$

The open circles in Fig. 1 represent a plot of the T_g-value versus the actual amorphous fraction of PCL obtained from Eq. (6), which fits the Fox equation quite well.

Fig. 1 also shows the T_c and T_m values of the quenched samples as a function of blend composition. Neither a crystallization exotherm nor a melting endotherm is observed in the blends with 80 wt% DGEBA or more, indicating that in these blends PCL has no tendency to crystallize during the quenching and the subsequent heating scan. For blends containing 70 wt% PCL or more, no crystallization exotherm is observed during heating since the crystallization of PCL is sufficiently rapid to be complete during the quenching. The blends with 30–60 wt% PCL display a crystallization exotherm during heating above their T_g; their T_c increases with increasing DGEBA content, indicating a progressively more difficult crystallization of PCL in these blends.

A decrease of the crystallization rate of PCL in the uncured DGEBA/PCL blends was also observed from the DSC thermograms of PCL and DGEBA/PCL blends at a cooling rate of −10°C/min from 100°C. The crystallization peak was observed to shift to lower temperatures with increasing DGEBA content, clearly indicating that the overall crystallization rate of PCL in the blends decreases with increasing DGEBA content. For the blend containing 10 wt% PCL, no crystallization exotherm was observed during the cooling run. The crystallization temperature of the cooling scan, T_c(cooling), is also shown in Fig. 1 as a function of composition. The decrease of the overall crystallization rate of PCL in the blend can be accounted for by the increase in the T_g of the blends with increasing DGEBA content resulting in lower molecular mobility, and hence a reduced crystallization rate of PCL in the blends. This result further supports the conclusion that DGEBA is completely miscible with PCL over the entire blend composition range in the melt.

The melting curve of PCL in the blends exhibits two peaks, which are both affected by melting point depression. The as-prepared samples display only one melting peak. It is believed that the double melting behavior in the quenched blends is the overall result of imperfect crystallization of PCL during quenching, giving rise to partial melting and recrystallization of PCL during heating.

It can clearly be seen from Fig. 1 that the T_m of PCL in the blends decreases with increasing DGEBA content. The T_m-depression is a common phenomenon for miscible blends containing one crystallizable component [25–27]. When the molecular weight of both components is sufficiently high, only the enthalpic contribution to the melting point depression is not negligible. In the present case, both enthalpic and entropic effects can contribute to the melting point depression in the uncured DGEBA/PCL blends owing to the low molecular weight of DGEBA. Morphological factors can also have an influence on the T_m of PCL.

The values of X_c(PCL) obtained for the uncured DGEBA/PCL blends are plotted in Fig. 2 as a function of blend composition. The X_c(PCL) values for the as-prepared samples are all higher than those for the quenched samples. For the quenched samples, X_c(PCL) is almost independent of PCL content down to 70 wt%, but then rapidly decreases at lower PCL content. For the as-prepared samples, X_c(PCL) remains nearly constant down to about 10 wt% PCL. Fig. 2 also illustrates the X_c(PCL) of the cooling scan as a function of composition; these values are immediate between those

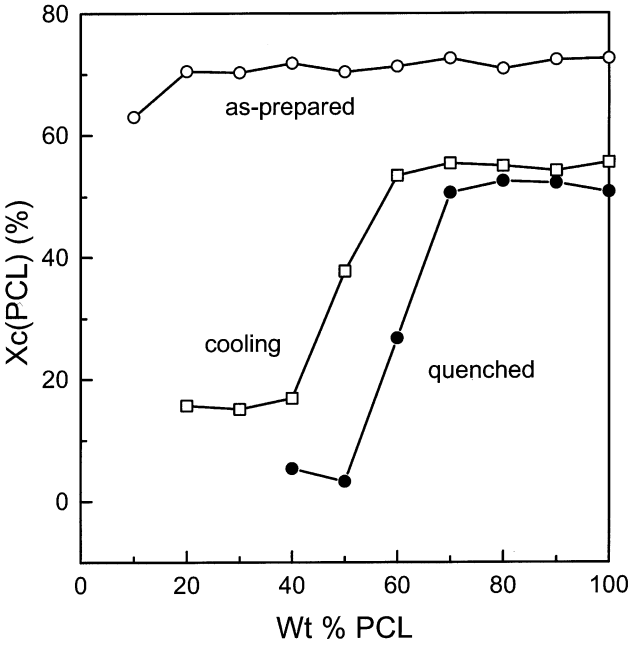

Fig. 2. X_c(PCL) versus PCL weight fraction of the uncured DGEBA/PCL blends. (○) As-prepared samples, (●) quenched samples, and (□) X_c(PCL) developed during the cooling scan.

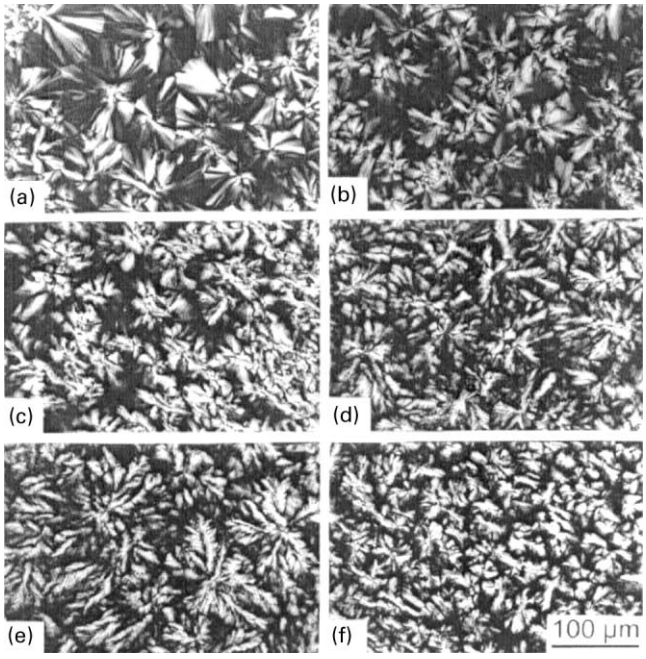

Fig. 3. Optical micrographs of uncured DGEBA/PCL blends isothermally crystallized at 40°C. DGEBA/PCL: (a) 10/90, (b) 30/70, (c) 40/60, (d) 50/50, (e) 60/40, and (f) 70/30.

of the as-prepared and the quenched samples. This indicates that the quenching process imposes great hindrance to the crystallization of the DGEBA/PCL blends and that the crystallization of the as-prepared samples is much more complete than that of the quenched samples on account of the slow cooling rate and long residence time at room temperature.

PCL spherulites were observed in the DGEBA/PCL blends with DGEBA content up to 70 wt%. Fig. 3 shows the optical micrographs of the DGEBA/PCL blends isothermally crystallized at 40°C. The blends with less than 30 wt% PCL are still completely volume-filled with spherulites, indicating the absence of interspherulitic segregation of DGEBA during the crystallization process. As the molecular weight of DGEBA is rather low, this phenomenon can be considered to be due to the low T_g (−11°C) of DGEBA and the rather high mobility of the DGEBA molecules at the crystallization temperature (40°C). It is also interesting that the spherulitic morphology becomes more irregular and coarser.

3.2. Miscibility and spherulitic morphology of MCDEA-cured ER/PCL blends

All MCDEA-cured ER/PCL blends were transparent just above the melting point of PCL indicating miscibility. Fig. 4 shows the thermal transition temperatures obtained from the DSC thermograms of the quenched samples of cured ER/PCL blends. The Gordon–Taylor equation [28] was used to describe the T_g-composition dependence:

$$T_g(\text{blend}) = (W(\text{PCL})T_g(\text{PCL}) + kW(\text{ER})T_g(\text{ER}))/(W(\text{PCL}) + kW(\text{ER})) \quad (7)$$

where k is a constant. The broken line in Fig. 4 corresponds to a k-value of 0.37. Note that, for the cured ER/PCL blends with 80 wt% or more PCL, the experimental values of T_g (full circles) display a remarkable positive deviation from those predicted by the Gordon–Taylor equation due to the high crystallinity of PCL. A plot of the T_g-values (open circles) versus the actual weight fraction of PCL in the amorphous phase, calculated using Eq. (6), fits the Gordon–Taylor equation quite well.

Fig. 4 also contains the T_c and T_m-values of the quenched samples as a function of the blend composition. Neither crystallization exotherm nor melting endotherm is observed in the blends with 40 wt% ER or more, indicating that PCL in these blends is unable to crystallize during quenching and subsequent heating. For the blends containing 80 wt% or more PCL, there is no crystallization exotherm during heating since the crystallization of PCL is sufficiently rapid to be complete during the quenching. The blends with 70 and 75 wt% PCL do display a distinct crystallization exotherm during heating above their T_g; the crystallization temperature (T_c) increases with increasing ER content,

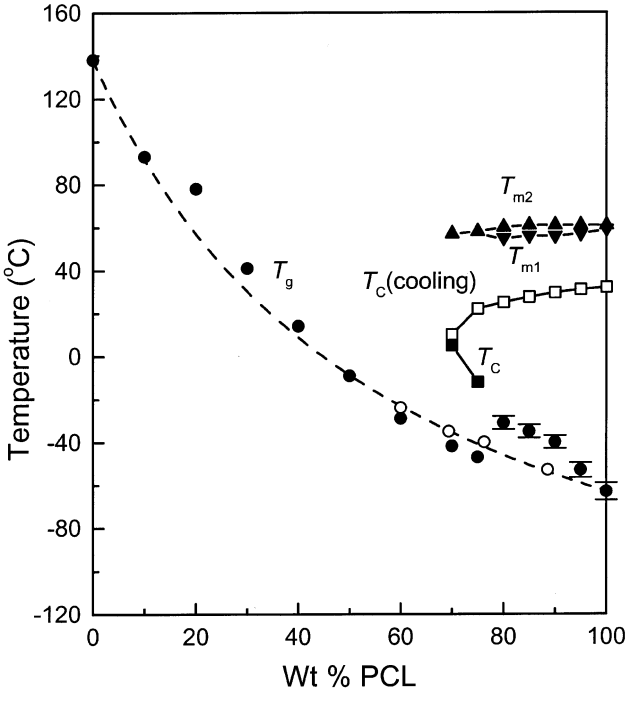

Fig. 4. Thermal transitions of the quenched samples of the MCDEA-cured ER/PCL blends. (●) Experimental T_g versus overall blend composition, (○) T_g versus calculated amorphous composition, (-----) theoretical curve of T_g versus blend composition as predicted by the Gordon–Taylor equation using a value of $k = 0.37$, and (□) T_c(cooling).

implying an increasingly difficult crystallization of PCL in the blends.

DSC thermograms of PCL and of the cured ER/PCL blends were obtained at a cooling rate of −10°C/min from 100°C. It was observed that the crystallization peak shifted to lower temperatures with increasing ER content, and there was no crystallization exotherm during the cooling run for the blends containing less than 70 wt% PCL. The crystallization temperature during the cooling scan, T_c(cooling), is plotted in Fig. 4 as a function of composition. The overall crystallization rate of PCL in the cured blends decreases much more rapidly with increasing ER content than that of the uncured DGEBA/PCL blends. This can be ascribed to the much higher T_g of the MCDEA-cured ER (138°C) compared to that of DGEBA (−11°C).

It can also be seen from Fig. 4 that the T_m of PCL in the quenched samples of the cured blends decreases slightly with increasing ER content; the T_m depression is, however, much less pronounced than that observed for the uncured DGEBA/PCL blends (Fig. 1). This is due to the fact that only the enthalpic contribution to the melting point depression plays a role for the MCDEA-cured ER/PCL blends.

The melting behavior of PCL in the quenched samples of the cured ER/PCL blends also exhibits two peaks. The difference between the two T_ms is much smaller than that for the uncured DGEBA/PCL blends. Melting point depression can be seen for both T_m's. For the as-prepared samples, only a single T_m was observed. The double melting point phenomenon in the quenched samples can thus be considered to result from the imperfect crystallization of PCL during quenching, leading to its partial melting and recrystallization during heating.

Fig. 5 shows the values of X_c(PCL) for the ER/PCL blends as a function of composition. The X_c(PCL)-values for the as-prepared samples are all higher than those for the quenched samples. For the quenched samples, X_c(PCL) remains almost constant for PCL contents down to 80 wt% and then sharply decreases with decreasing PCL content. For the as-prepared samples, X_c(PCL) gradually decreases between 100 and 40 wt% PCL content. This clearly indicates that the quenching process imposes great hindrance to the crystallization of the ER/PCL blends, and that the crystallization of the as-prepared samples is much more complete than that of the quenched samples. The crystallinity of PCL in the cured ER/PCL blends decreases much more rapidly with increasing amorphous ER content than that of the uncured DGEBA/PCL blends (Fig. 2); this can also be accounted for by the much higher T_g of the MCDEA-cured ER.

PCL spherulites were observed in the cured ER/PCL blends with ER content up to 50 wt%. Fig. 6 shows the optical micrographs of these blends isothermally crystallized at 40°C. The blends with PCL content down to 50 wt% are still completely volume-filled with spherulites, and the size of the spherulites gradually decreases with ER content beyond 10 wt%. The spherulitic morphology appears to remain unchanged with ER content up to 50 wt% (i.e. it does not become more irregular or coarser). This means that there is no interspherulitic segregation of MCDEA-cured ER, the amorphous cured ER molecules must be segregated

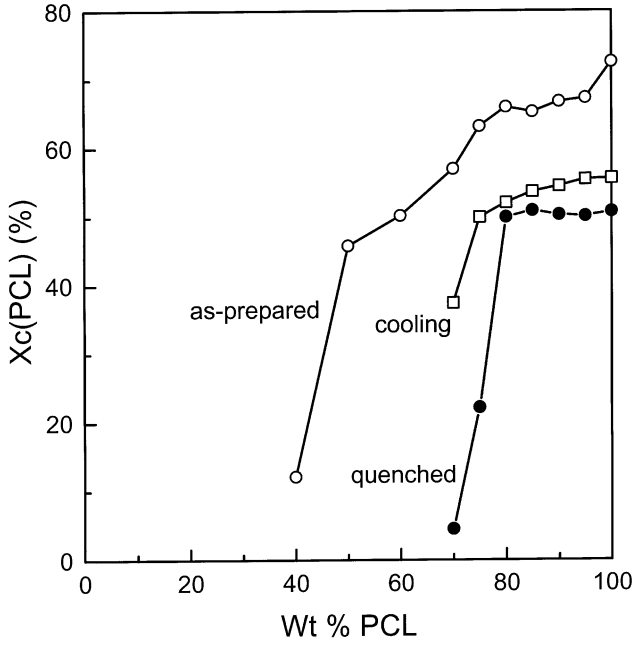

Fig. 5. X_c(PCL) versus PCL weight fraction of the MCDEA-cured ER/PCL blends. (○) As-prepared samples, (●) quenched samples, and (□) X_c (PCL) developed during the cooling scan.

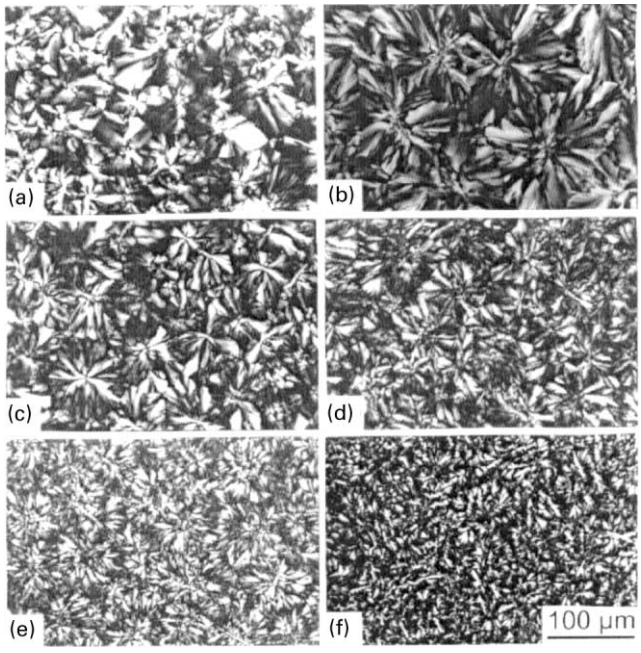

Fig. 6. Optical micrographs of the MCDEA-cured ER/PCL blends isothermally crystallized at 40°C. ER/PCL: (a) 0/100, (b) 10/90, (c) 20/80, (d) 30/70, (e) 40/60, and (f) 50/50.

interlamellarly or interfibrillarly during the crystallization of PCL.

3.3. Hydrogen-bonding interactions in MCDEA-cured ER/PCL blends

From the thermodynamic point of view, an increase in molecular weight for either component of a miscible blend will reduce the entropy of mixing. This, together with the usually positive (endothermic) enthalpy of mixing, will result in phase separation. Therefore, the occurrence of miscibility in polymer blends containing one component with an infinite molecular weight (i.e. highly crosslinked) requires a negative (exothermic) enthalpy of mixing [2].

PCL has been shown to exhibit miscibility with many other polymers due to its high propensity to form hydrogen bonds with these polymers [27,29–35]. In particular, it has been proven that there is hydrogen bonding between PCL and poly(hydroxyether of bisphenol A) (phenoxy) [32], and PCL was found to be miscible with phenoxy [32,33]. It should be pointed out that phenoxy can be considered as a linear model bisphenol A-type epoxy resin, i.e. linear high-molecular-weight polymer of DGEBA.

Although the DGEBA sample used contains only a small amount of hydroxyl groups, the curing reaction between epoxy groups and amine groups will result in the formation of hydroxyl groups in the MCDEA-cured ER molecules which can form a large number of hydrogen bonds with the carbonyl groups of PCL. FTIR studies revealed that hydrogen bonding in the cured blends occurs between the hydroxyl groups of MCDEA-cured ER and the carbonyl groups of PCL. There are two areas of interest in the infrared spectra of the blends, one is the hydroxyl stretching region from 3600 to 3000 cm^{-1} and the other is the carbonyl stretching region from 1800 to 1650 cm^{-1}.

Fig. 7 shows the FTIR spectra of the MCDEA-cured ER/PCL blends in the stretching region of the ER hydroxyl groups ranging from 3000 to 3800 cm^{-1}. The spectrum of the pure MCDEA-cured ER in this region may be considered to have two components; a broad band centered at 3417 cm^{-1} attributed to the self-associated hydroxyl, i.e. hydrogen bonded hydroxyl groups, and another relatively narrow band at 3557 cm^{-1} assigned to non-associated, free hydroxyl groups. In the blends with PCL, the non-associated hydroxyl band at 3557 cm^{-1} does not shift. In contrast, the associated hydroxyl band at 3417 cm^{-1} shifts to higher frequencies with increasing PCL concentration, indicating that there is hydrogen bonding between the hydroxyl groups of ER and the carbonyl groups of PCL. The intensity ratio between the hydrogen bonded hydroxyl band and the free hydroxyl band increases with increasing PCL concentration, indicating the gradual increase of the fraction of hydrogen bonded hydroxyls in the blends. The frequency difference between the free hydroxyl absorption and that of the hydrogen bonded species ($\Delta\nu$) is a measure of the average strength of the intermolecular interactions [36]. Therefore,

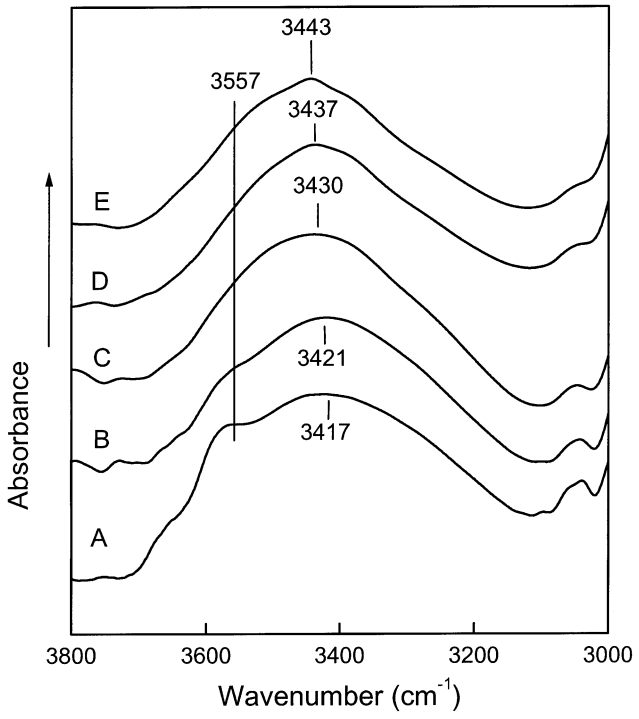

Fig. 7. FTIR spectra in the 3000–3800 cm^{-1} region of the MCDEA-cured ER/PCL blends. ER/PCL: (A) 100/0, (B) 90/10, (C) 70/30, (D) 50/50, and (E) 30/70.

the above results indicate that the average strength of the hydrogen bond between the hydroxyl groups of ER and the carbonyl groups of PCL in the cured blends ($\Delta\nu =$ 114 cm^{-1} for the cured 30/70 ER/PCL blend) is lower than that between the hydroxyl groups in the pure cured ER ($\Delta\nu = 140\ cm^{-1}$). Similar results have been observed by other investigators. Coleman et al. [34]found that the average strength of the hydrogen bond between the PCL carbonyl group and the poly(*p*-vinyl phenol) (PVPh) hydroxyl group ($\Delta\nu = 105\ cm^{-1}$) is less than that occurring between the hydroxyl groups in plain PVPh ($\Delta\nu =$ 165 cm^{-1}) in the PVPh/PCL system. The average strength of the hydrogen bond between the PCL carbonyl group and the hydroxyl group of phenoxy ($\Delta\nu = 90\ cm^{-1}$) is less than that between the hydroxyl groups in plain phenoxy ($\Delta\nu =$ 170 cm^{-1}) in the phenoxy/PCL system [35].

Fig. 8 shows the FTIR spectra of the MCDEA-cured ER/PCL blends between the 1600 and 1850 cm^{-1}, corresponding to the stretching vibration of the carbonyl groups of PCL. The carbonyl stretching vibration band of pure PCL is at 1726 cm^{-1}. Upon blending with ER, a second band develops at 1707 cm^{-1} corresponding to the hydrogen-bonded carbonyl groups and its intensity relative to that of the free carbonyl groups band slightly increases with increasing ER concentration. This is also indicative of hydrogen bonding between the hydroxyl groups of ER and the carbonyl groups of PCL.

From the analysis of the FTIR spectra, it is believed that hydrogen-bonding interaction is an important driving force

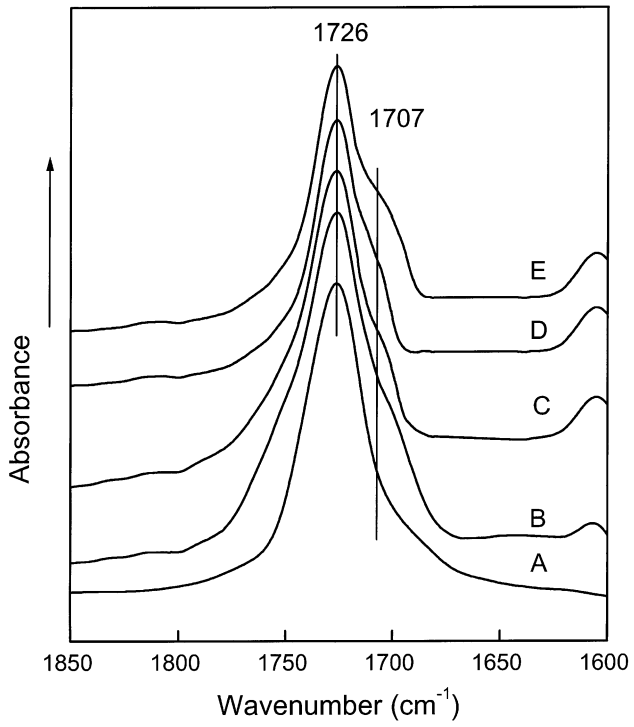

Fig. 8. FTIR spectra in the 1600–1850 cm^{-1} region of the MCDEA-cured ER/PCL blends. ER/PCL: (A) 0/100, (B) 10/90, (C) 30/70, (D) 50/50, and (E) 70/30.

for the miscibility of the ER/PCL blends. The results further confirm that the MCDEA-cured ER/PCL blends are completely miscible.

3.4. Real-time SAXS investigation of the semicrystalline morphology of MCDEA-Cured ER/PCL blends

Crystallization in a miscible blend involves diffusion of the crystallizable component towards the crystallization front and rejection of the non-crystallizable component. The liquid–solid phase separation occurring during the crystallization process of PCL in miscible MCDEA-cured ER/PCL blends requires the segregation and diffusion of amorphous cured ER away from the crystalline nucleus. The cured ER molecules have a rather limited mobility as compared with the linear polymer diluents.

The semicrystalline morphology of PCL in some of its miscible blends with linear polymers such as poly(vinyl chloride) [37–39], poly(styrene-*co*-maleic anhydride) [40], and phenoxy [41] has been investigated by SAXS. Real-time SAXS was measured for samples of plain PCL and 10/90, 20/80, 25/75 MCDEA-cured ER/PCL blends.

Fig. 9 shows Lorentz-corrected and smoothed real-time SAXS patterns of a 10/90 cured ER/PCL blend during cooling from 80 to 25°C at −10°C/min (Fig. 9(a)) and during the subsequent heating from 25 to 80°C at 10°C/min (Fig. 9(b)). Fig. 9(a) illustrates that a maximum of scattering intensity appears at low temperatures during cooling, indicating crystallization

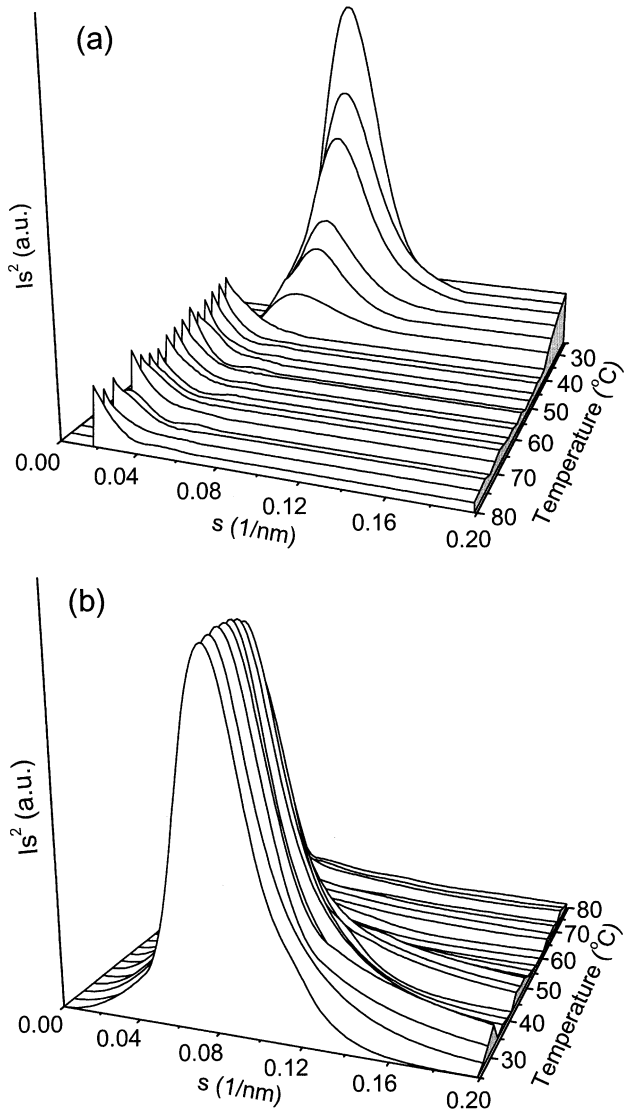

Fig. 9. Lorentz corrected SAXS patterns of a 10/90 MCDEA-cured ER/PCL blend during (a) cooling at −10°C/min from 80 to 25°C and (b) subsequent heating at 10°C/min from 25 to 80°C after the cooling. The spikes in the curves are artifacts due to spline smoothing.

of PCL in the blend. The maximum of scattering intensity disappears, however, at high temperatures during the subsequent heating as shown in Fig. 9(b).

Linear correlation functions [23] were calculated from the SAXS patterns obtained during heating for the plain PCL and the blends. Fig. 10 gives an example of linear correlation functions calculated from the SAXS patterns of the 10/90 cured ER/PCL blend during the heating, which clearly illustrates the evolution of the long period. Fig. 11 gives morphological parameters obtained from the correlation functions as a function of temperature below 55°C for the plain PCL and the three blends studied. The long period L and amorphous layer thickness l_a substantially increase with increasing temperature. In contrast, the lamellar layer thickness l_c only slightly increases with temperature.

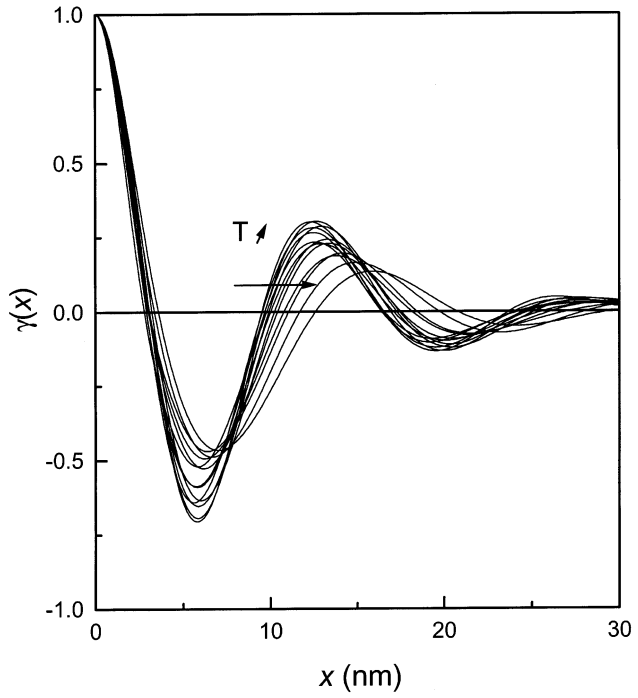

Fig. 10. Linear correlation functions during heating at 10°C/min from 25 to 80°C of a 10/90 MCDEA-cured ER/PCL blend after the cooling.

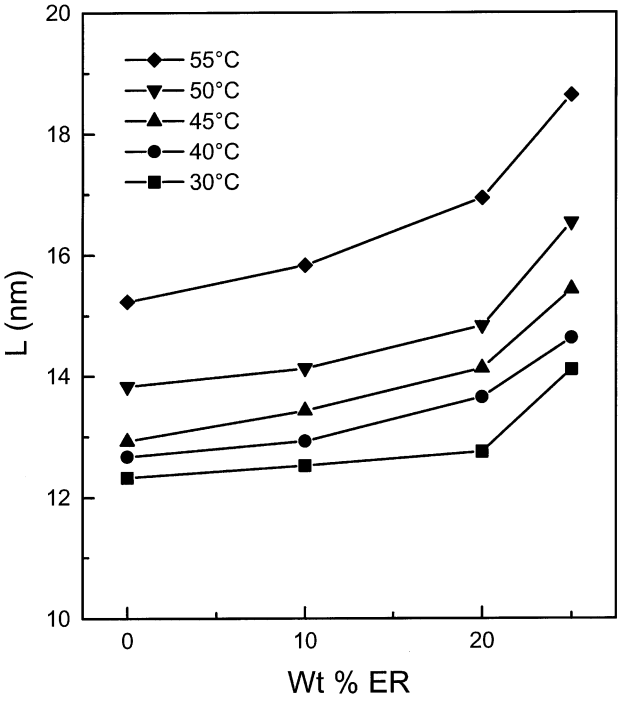

Fig. 12. Long period, L, as a function of composition for MCDEA-cured ER/PCL blends.

Fig. 12 shows the long period L as a function of blend composition at various temperatures. The long period L increases drastically with increasing ER content, suggesting that interlamellar segregation occurs in the cured ER/PCL blends. Fig. 13 shows both the lamellar layer thickness l_c and amorphous layer thickness l_a as a function of composition. The lamellar layer thickness l_c slightly decreases with increasing ER content whereas the amorphous layer thickness l_a increases dramatically. The value of l_a is very important with respect to the understanding of the segregation behavior of the amorphous component in a semicrystalline blend and interlamellar segregation can be detected with SAXS from an increase in the amorphous layer thickness [40–43]. It is clear that the amorphous cured ER molecules segregate interlamellarly during the crystallization of PCL.

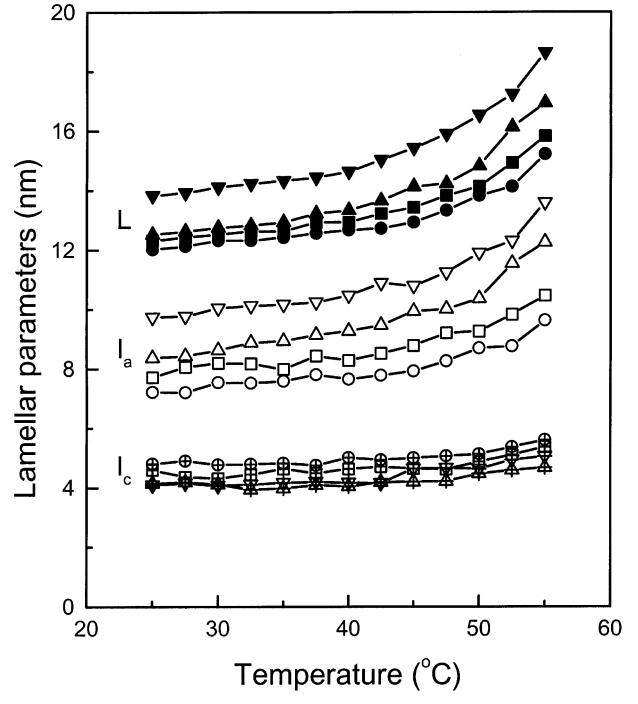

Fig. 11. Variation of lamellar parameters as a function of temperature for MCDEA-cured ER/PCL blends during (a) heating at 10°C/min from 25 to 80°C. ER/PCL: (a) circles: 0/100, (b) squares: 10/90, (c) up triangles: 20/80, and (b) down triangles: 25/75.

The occurrence of interlamellar segregation in the cured ER/PCL blend can be fully understood if one considers the low chain mobility of the cured ER in the ER/PCL blends. The cured ER molecules diffuse away slowly from the crystallization nucleus, as compared to the usual linear diluent polymers in blends with PCL. The low chain flexibility and high T_g could be responsible for the hindered diffusion process. It remains difficult to imagine the segregation process of the ER network in the blend during the crystallization of PCL. The topology of the network of crosslinked component ER should have a considerable influence on the crystallization and segregation. For the blends with PCL content above 75 wt%, the curing reaction can hardly be complete. In order to avoid thermal degradation of PCL, the curing temperatures were not sufficiently high, and the ER hence also not sufficiently cured in the blends. Curing reactions involve chain extension, branching and crosslinking. As the curing reactions proceed, the molecular weight of the system drastically increases. The crosslink density of the epoxy network should also depend on the blend composition.

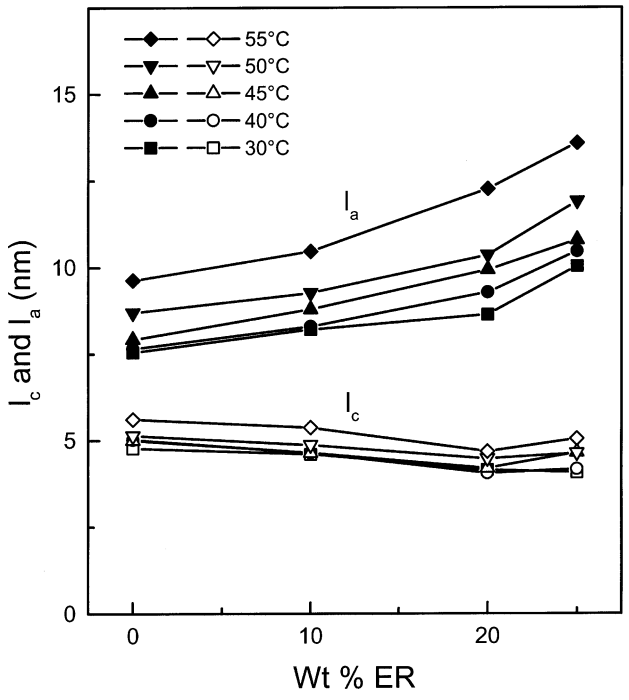

Fig. 13. Lamellar thickness, l_c, and amorphous thickness, l_a, as a function of composition for MCDEA-cured ER/PCL blends.

For blends with low PCL content, a three-dimensional crosslinking network structure forms; and the blends display a homogeneous semi-interpenetrating network (semi-IPN) structure. In this semi-IPN, the initially miscible components still exhibit characteristics of miscibility because of favorable hydrogen-bonding interactions. In contrast, for blends with low ER content, only highly branched chain molecules and an imperfect network are formed. This type of cured ER molecules has a very limited mobility and can diffuse only very slowly away from the crystallization.

Fig. 14 schematically illustrates a model of the structure of a cured ER/PCL blend in the miscible melt and the lamellar structure of a crystallized blend. In the melt, PCL is miscible with the highly branched ER molecules and imperfect ER network, and the blend has a homogeneous structure. In the crystallized blend, the semicrystalline morphology corresponds to a stack of crystalline lamellae with the amorphous fraction of PCL, the branched ER chains and imperfect ER network located between PCL lamellae. The highly branched ER chains and the imperfect ER network are segregated interlamellarly during crystallization of PCL in the MCDEA-cured ER/PCL blends.

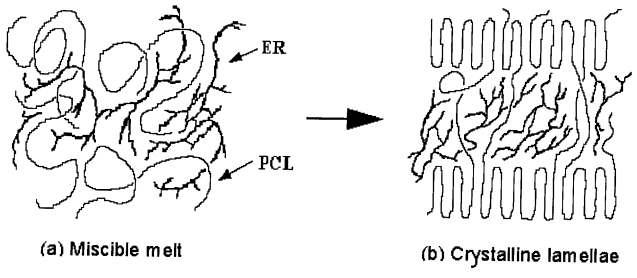

Fig. 14. Model describing (a) the miscible melt and (b) the crystalline lamellae of the MCDEA-cured ER/PCL blends.

4. Conclusions

Both the uncured DGEBA/PCL blends and the MCDEA-cured ER/PCL blends are completely miscible over the entire composition range. The overall crystallization rate and crystallinity of PCL in the cured ER/PCL blends decrease much more rapidly with increasing amorphous ER content than the uncured DGEBA/PCL blends. This is due to the higher T_g of the cured blends. The spherulitic morphology of PCL in both the DGEBA/PCL blends and the cured ER/PCL blends shows typical characteristics of miscible crystalline/amorphous blends, and the PCL spherulites are always completely volume-filling. The miscibility of the uncured DGEBA/PCL blends is predominately due to the entropic contribution, whereas the miscibility of the cured ER/PCL blends is due to the enthalpic contribution. Hydrogen-bonding between the hydroxyl groups of MCDEA-cured ER and the carbonyl groups of PCL is responsible for the miscibility in the cured blends. The average strength of the hydrogen bond in the cured ER/PCL blends is lower than that in the pure cured ER. During crystallization of PCL, the amorphous cured ER molecules segregate interlamellarly. The occurrence of interlamellar segregation in the cured ER/PCL blend is ascribed to the low chain mobility of the cured ER in the ER/PCL blends. The amorphous fraction of PCL, the branched ER chains and imperfect ER network are located between PCL lamellae. The highly branched ER chains and the imperfect ER network are segregated interlamellarly during crystallization of PCL.

Acknowledgements

The authors are indebted to Dr F. Defoor, Shell Research, Louvain-la-Neuve, Belgium, for kindly supplying the Epikote 828EL sample and to the Fund for Scientific Research Flanders (F.W.O.-Vlaanderen). One of us (Q.G.) wishes to express his appreciation to the KULeuven Research Council for awarding a Senior Fellowship for Visiting Professors. This work was supported under the TMR/LSF program of the European Commission (contract ERBFMGECT980134).

References

[1] Ultracki LA. Polymer alloys and blends. Munich: Hanser Publishers, 1989.

[2] Guo Q. In: Shonaike GO, Simon G, editors. Polymer blends and alloys. New York: Marcel Dekker, 1999. p. 155–87 (chap. 6).
[3] Noshay A, Robeson LM. J Polym Sci, Polym Chem Ed 1974;12:689.
[4] Clark JN, Daly JH, Garton A. J Appl Polym Sci 1984;9:3381.
[5] Guo Q, Peng X, Wang Z. Polym Bull 1989;21:593.
[6] Guo Q, Peng X, Wang Z. Polymer 1991;32:53.
[7] Widmaier JM. Macromolecules 1991;24:4209.
[8] Ramesh P, De SK. J Appl Polym Sci 1993;50:1369.
[9] Guo Q, Zheng H. Polymer 1999;40:637.
[10] Zhang X, Solomon DH. Macromolecules 1994;27:4919.
[11] Mucha M. Colloid Polym Sci 1994;272:1090.
[12] Luo X, Zheng S, Zhang N, Ma D. Polymer 1994;35:2619.
[13] Zheng H, Zheng S, Guo Q. J Polym Sci, Polym Chem Ed 1997;35:3161.
[14] Zheng H, Zheng S, Guo Q. J Polym Sci, Polym Chem Ed 1997;35:3169.
[15] Zhong Z, Guo Q. Polymer 1998;39:517.
[16] Bauser RS, editor. Epoxy resin chemistry II ACS symposium series, No. 201. Washington DC: American Chemical Society, 1983.
[17] Riew CK, Kinloch AJ, editors. Toughened plastics I: science and engineering ACS symposium series, no. 233. Washington DC: American Chemical Society, 1993.
[18] Guo Q. Polymer 1993;34:70.
[19] Koch MHJ, Bordas J. Nucl Instrum Meth 1983;208:461.
[20] Boulin CJ, Kempf R, Koch MHJ, McLaughlin SM. Nucl Instrum Meth 1986;A249:399.
[21] Strobl G, Schneider MJ. J Polym Sci, Polym Phys Ed 1980;18:1343.
[22] Fox TG. Bull Am Phys Soc 1956;1:123.
[23] Crescenzi V, Manzini G, Calzolari G, Borri C. Eur Polym J 1972;8:449.
[24] Fernandes AC, Barlow JW, Paul DR. J Appl Polym Sci 1984;29:3381.
[25] Nishi T, Wang TT. Macromolecules 1975;8:909.
[26] Imken RL, Paul DR, Barlow JW. Polym Engng Sci 1976;16:593.
[27] Defieuw G, Groeninckx G, Reynaers H. Polymer 1989;30:595.
[28] Gordon M, Taylor JS. J Appl Chem 1952;2:495.
[29] Ong CJ, Price FP. J Polym Sci, Polym Symp 1978;63:45 (see also page 59).
[30] Belorgey G, Prud'homme ER. J Polym Sci, Polym Phys Ed 1982;20:191.
[31] Guo Q. Makromol Chem 1990;191:2639.
[32] Brode GL, Koleske JV. J Macromol Sci, Chem 1992;A6:1109.
[33] Robeson LM, Hale WF, Merriam CN. Macromolecules 1981;14:1644.
[34] Coleman MM, Moskala E. J Polym 1983;24:251.
[35] Moskala EJ, Varnell DF, Coleman MM. Polymer 1985;26:228.
[36] Purcell KF, Drago RS. J Am Chem Soc 1968;89:2874.
[37] Warner FP, MacKnight WJ, Stein RS. J Polym Sci, Polym Phys Ed 1977;15:2113.
[38] Russell TP, Stein RS. J Macromol Sci 1980;Bl7:617.
[39] Nojima S, Tsutsui H, Urushihara M, Kosaka W, Kato N, Ashida T. Polym J 1986;18:451.
[40] Defieuw G, Groeninckx G, Reynaers H. Polymer 1989;30:2158.
[41] Defieuw G, Groeninckx G, Reynaers H. Polymer 1989;30:2164.
[42] Dreezen G, Koch MHJ, Reynaers H, Groeninckx G. Polymer 1999;40:6451.
[43] Dreezen G, Mischenko N, Koch MHJ, Reynaers H, Groeninckx G. Macromolecules 1999;32:4015.